Università degli Studi dell'Aquila
Dipartimento di Ingegneria Civile, Edile-Architettura e Ambientale

SAPIENZA
UNIVERSITÀ DI ROMA

ISSN 2612-4009

DYNAMIC INTERACTION OF SOIL AND STRUCTURE (DISS_15)

THE 4th INTERNATIONAL WORKSHOP

"Archaeology, Cryptoportici, Hypogea, Geology, Geotechnics, Geophysics"

Rome, 12-13 November 2015

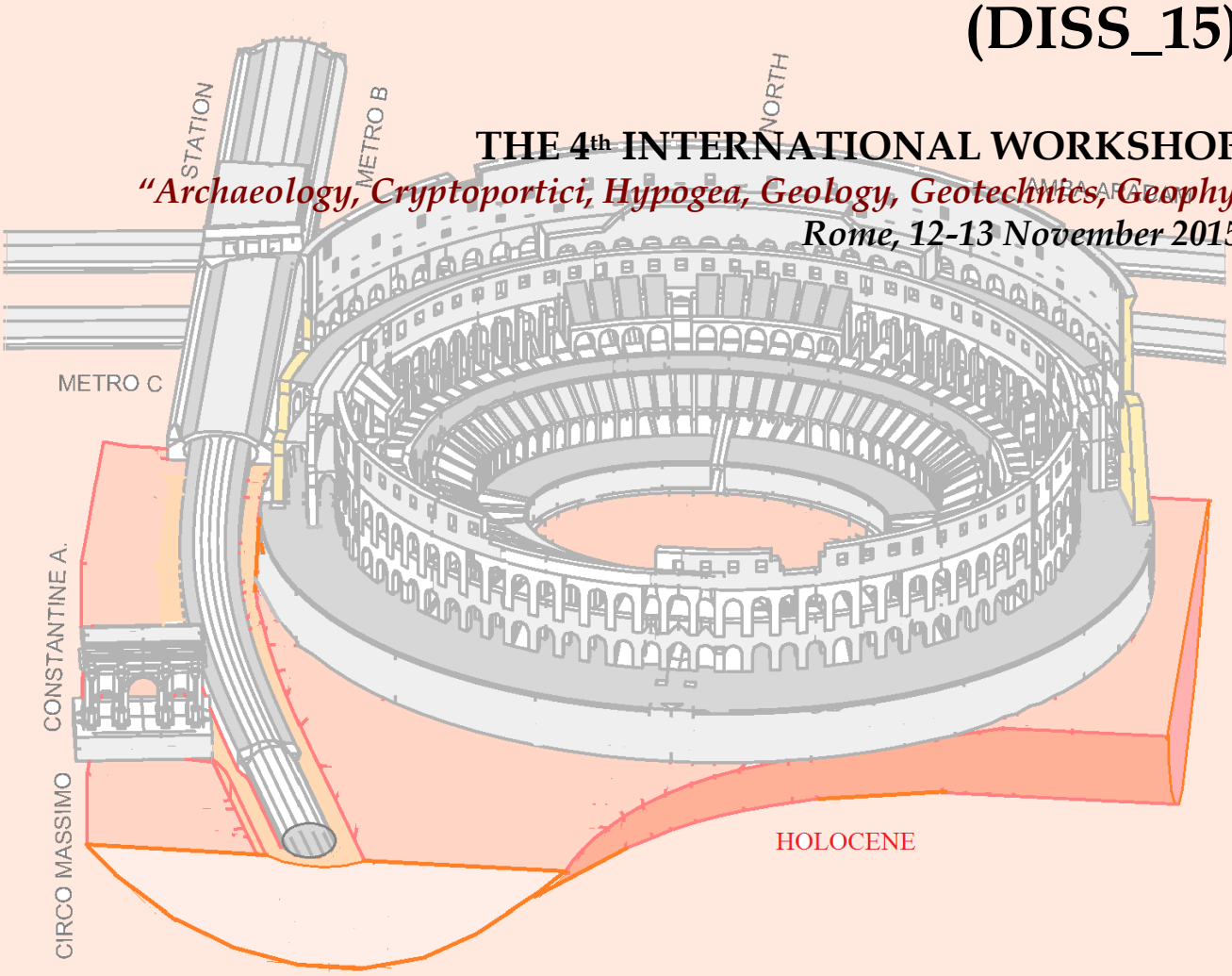

Proceedings of the 4th International Workshop on "Dynamic Interaction of Soil and Structure (DISS_15)"

"Archaeology, Cryptoportici, Hypogea, Geology, Geotechnics, Geophysics"

Rome, 12-13 November 2015

DISS_*Edition* c/o DICEAA - L'Aquila University - via Giovanni Gronchi, 18
67040 L'Aquila - +39.0862.434552
www.diss-co.it – info@diss-co.it

1st edition: July 2016

ISSN 2612-4009

ISBN 978-88-940114-2-

In the same collection, Proceedings of the International Workshops "*Dynamic Interaction of Soil and Structure"*:

1st DISS_10, L'Aquila 19 March 2010, D'Ovidio G., Nakamura Y., Rovelli A., Valente G., Aracne, ISBN 978-88-548-3693-8.

2nd DISS_12, L'Aquila 29-30 March 2012, Clemente P., D'Ovidio G., Nakamura Y., Rovelli A., Tallini M., Totani G., Valente G., DISS_*Edition*, ISBN 978-88-94011-0-1.

3rd DISS_13, Rome 12-13 December 2013, Carlo Baggio, Paolo Clemente, Yutaka Nakamura, Luciana Orlando, Antonio Rovelli, Gianfranco Valente, DISS_*Edition*, ISBN 978-88-94011418.

SECRETARIAT: Aitef Studio s.r.l., Via Thailandia, 27 – 00144 Rome, Italy – www.aitefstudio.it

DYNAMIC INTERACTION OF SOIL AND STRUCTURE (DISS_15)

PROCEEDINGS OF THE 4th INTERNATIONAL WORKSHOP
"Archaeology, Cryptoportici, Hypogea, Geology, Geotechnics, Geophysics"
ROME, 12-13 NOVEMBER 2015

WORKSHOP CHAIRMEN
Giorgio Monti, Gianfranco Valente

Some aspects of the seismic behaviour of a large homogeneous earth dam

Luca Masini[1], Sebastiano Rampello[1], Luigi Callisto[1]

Abstract

Instability phenomena of large existing earth dams are one of the major source of seismic vulnerability in Italy, as most of them were constructed in the absence of specific seismic regulations. Therefore, it is necessary to investigate the response of such earth structures when subjected to severe earthquake loading, estimating the safety conditions with respect to deformation phenomena which can compromise the water retention capability.

This paper discusses some results of a study on the seismic behaviour of a large homogeneous earth dam. Specifically, monitoring data taken during construction and impounding of the dam were used to calibrate a plane-strain numerical model. Iterative pseudo-static analyses were first conducted by uniformly accelerating the finite-difference model to investigate the plastic mechanisms forming under critical conditions. The seismic performance of the dam was then evaluated through a series of dynamic analyses in which a real seismic record was used as input motion. In the analyses, the effects of the bedrock deformability and of the presence of the vertical component of the seismic action were investigated.

The results of the dynamic analyses evidenced that a significant reduction of the seismic energy is obtained if the deformability of the bedrock is accounted for, resulting in much lower permanent displacements of the embankment. Conversely, the vertical component of the seismic action induces a sensible increase of the seismic displacements, so that analyses conducted neglecting the vertical component of the ground motion can lead to an unsafe evaluation of the water retention capability.

---

1 “Sapienza” University of Rome, Italy.

1. Model calibration

The seismic behaviour of large earth dams is strongly affected by the inertial forces that develop during the ground motion, changing with time and space. The distribution and evolution of these forces depend on the mechanical properties of the embankment and the foundation soil, the effective stress state induced by the construction and impounding stages as well as on the geometry of the dam. The effects of an earthquakes onto an earth dam derive also from a possible reduction in the shear strength of the dam body. This last phenomenon may be caused by the positive excess pore pressure developing in the saturated portion of the embankment in undrained conditions, and by the degradation of strength parameters under cyclic loading.
This study focuses on the seismic behaviour of the Marana Capacciotti dam, a large homogeneous earth dam located in Southern Italy [1,2,3,4,5]. A numerical model was conceived for the dam adopting some simplifying assumption about its geometry. This dam was selected in that a comprehensive geotechnical characterisation of the embankment and the foundation soil, as well as the monitoring data of the construction and the impounding stages are available from a previous study [1].

Figure 1 shows the simplified cross section of the embankment that was converted into a plane-strain numerical model. The dam has a height $H = 50$ m, a width of 400 m and the slope of the flanks is $\alpha = 14°$. The drainage system consists of a sub-vertical central drain and of a horizontal drain located at the toe of the downstream slope. An impervious diaphragm extending into the lower firm soil prevents seepage through the 15 m high alluvial deposit underlying the dam.

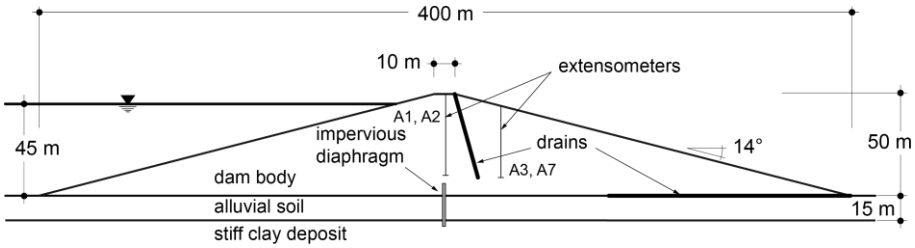

***Figure 1**. Simplified cross section of the dam and location of the extensometers*

***Table 1**. Mechanical soil properties*

soil	γ (kN/m³)	c' (kPa)	φ' (°)	ψ (°)	k_0 (-)	k (m/s)	A (MPa)	B (MPa)	n	ν
dam body	20.8	20	28	0	-	10^{-7}	19.476	1573	0.75	0.30
foundation soil	20.6	7	32	0	1.5	10^{-6}	19.476	2155	0.73	0.32
firm soil	20.6	-	-	-	1.5	10^{-9}	2060	0	-	0.32

The numerical analyses were carried out in terms of effective stresses using the finite difference code FLAC v.5.0 [6]. The soil was modelled as an elastic-perfectly plastic materials with Mohr-Coulomb's plasticity criterion and zero dilatancy. The strength and stiffness parameters of the soils were obtained from the geotechnical investigations carried out throughout the earth dam and in the foundation soils, as comprehensively reported by Calabresi *et al.* [1]. Table 1 lists the shear strength parameters obtained from standard consolidated undrained triaxial compression tests and drained direct shear tests. The small-strain shear modulus G_0 was expressed as a function of the mean effective stress p':

$$G_0 = A + B \cdot \left(\frac{p'}{p_{\text{ref}}} \right)^n \tag{1}$$

where p_{ref} = 1 kPa is a reference pressure. Values of coefficients A, B, and n were selected to match the measurements of G_0 obtained from resonant column tests carried out on the undisturbed samples retrieved from the dam body and the foundation soil. The stiff clay deposit found underneath the alluvial layer was regarded as a bedrock characterised by a shear wave velocity V_s = 1000 m/s, with constant values of small-train shear modulus G_0 = 2060 MPa and bulk modulus K = 5026.4 MPa.

The numerical model was initialised by simulating the static construction of the dam, the impoundment stages and the unconfined seepage through the embankment, to obtain a correct initial state of effective stress prior to the dynamic calculation. This is needed to calculate the G_0 distribution within the embankment and the foundation soil. The staged construction of the dam, considered as a drained process, was modelled by progressively activating 13 rows of zones about 4m thick, while the impounding of the reservoir to the maximum storage level of 45 m and the associated steady-state seepage flow through the dam were simulated by raising the water level in three steps of 15 m

each. The shear stiffness adopted for the static calculations was obtained reducing the small-strain shear stiffness G_0 by a factor which was calibrated to reproduce the settlement profiles observed during the construction stages. Specifically, an operative shear modulus G equal to 5% of G_0 was used for the dam body and the foundation soil, while a much lower value equal to 0.5% of G_0 was used for the firm soil. Such a large reduction was needed to reproduce the settlements measured at the base of the dam after the end of construction, in that the stiff clay deposit, here modelled as 2 a meters thick layer, has an estimated thickness of about 300 m. At the end of each static phase, the soil stiffness was updated according to Eq. (1) to be consistent with the new effective stress state. Model calibration was checked using the settlements measured during dam construction via four extensometers installed at the centreline and in the downstream slope of the dam, as shown in Figure 1. Figure 2 shows the settlement profiles of the dam body relative to its base, measured along two vertical axes through the crest of the dam (A1 and A2 in Fig. 2a), and two vertical axes located in the downstream slope (A3 and A7 in Fig. 2b), at a stage when the dam was not yet completed (H = 34m) and at the end of construction. The results of the numerical analysis, also plotted in the figures, are in a fair agreement with the monitoring data. The increase in settlements at the top of extensometers A3 and A7, observed at the end of construction can be attributed to the construction of the overlying portion of the dam.

2. Dynamic analyses

2.1. Free-field 1D seismic response analysis

The dynamic response of the numerical model was preliminarily calibrated by comparing the results of free-field 1D FLAC simulations with those obtained using the code MARTA v.1.1.06 [7], in which the soil is modelled as an nonlinear viscous-elastic material. To this aim, the seismic response of a 67 m height column of soil was studied, corresponding to the soil sequence at the dam centreline: from the top of the column, the first 50 m thick layer is composed by the dam body resting over the foundation soil, which consists of an alluvial deposit

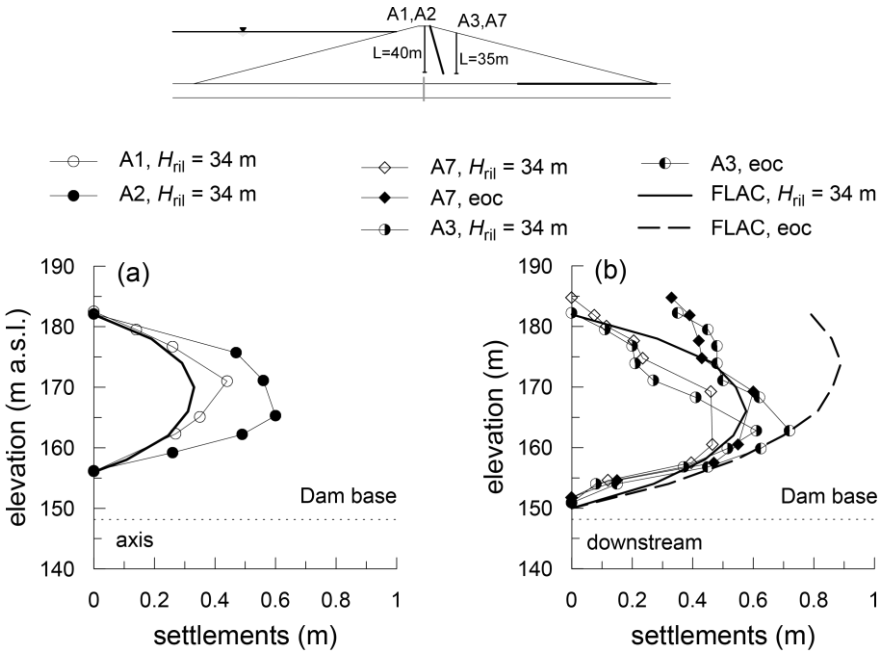

***Figure 2**. Observed and computed settlement profile.*

15 m thick overlying the bedrock, modelled as an elastic layer with a thickness of 2 m.

In the dynamic analyses, the cyclic behaviour of the dam body and the foundation soil was described through the hysteretic damping model Sigmoidal4, implemented in FLAC. This is an extension to two dimensions of the non-linear soil models that describe the unloading–reloading stress–strain cycles using Masing's rules. The model requires the value of the small-strain shear stiffness G_0 and a backbone curve. As discussed above, G_0 was expressed as a function of the mean effective stress (Eq. 1), while the backbone curve was calibrated to reproduce the modulus decay curves obtained from the resonant column (RC) tests performed on undisturbed samples retrieved from the embankment and the foundation soil. Figure 3 shows a comparison between the prediction of the hysteretic model and the modulus decay curves obtained from the RC tests on the samples retrieved from the dam body. The equation proposed by Ishibashi and Zang [8] is also plotted in the figure assuming a mean effective stress p' = 50 kPa and

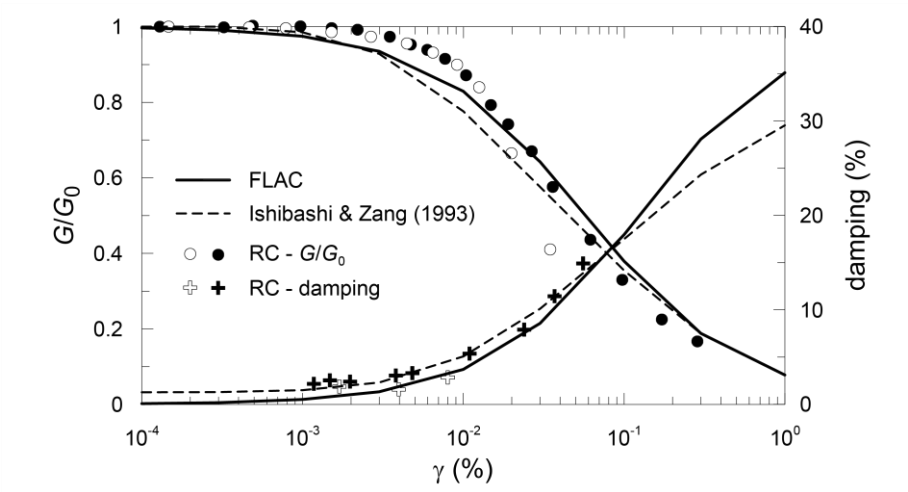

***Figure 3**. Comparison between RC tests results and model simulations.*

a plasticity index PI = 0. Table 1 lists the values of the strength and stiffness parameters adopted in the analyses.

A small amount of additional damping was introduced in the analyses to attenuate the soil response at very small strains and to reduce spurious high-frequency noise. This was obtained by specifying a FLAC frequency independent "local" damping ratio equal to 0.5%.

A real seismic record was used as input motion, selected from a set of events compatible with the seismicity of the site [2]. Specifically, the horizontal North-South and the vertical components of Tolmezzo record (Friuli 1976 earthquake) were used. In the 2D-simulations, the acceleration time histories were multiplied by a scaling factor $F = 1.8$ to match the elastic response spectrum of the newly-released Italian building code for dams [9], calculated for a return period $T_R = 2475$ years.

***Table 2**. Properties of the seismic input records*

record	a_{max} (*g*)	I_a (m/s)	T_s (s)	T_m (s)
Tolmezzo NS (*F*=1)	0.357	0.790	4.31	0.393
Tolmezzo V (*F*=1)	0.267	0.334	5.16	0.211
Tolmezzo NS (*F*=1.8)	0.642	2.561	4.31	0.393
Tolmezzo V (F=1.8)	0.480	1.084	5.16	0.211

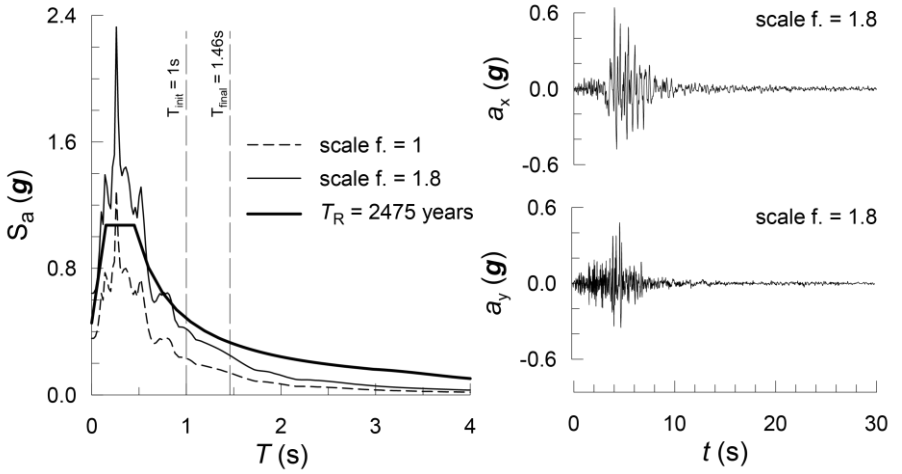

Figure 4. *Elastic response spectra and acceleration time histories of the input motion.*

Some properties of the records are reported in Table 2, where a_{max} is the peak ground acceleration, I_A is the Arias intensity, T_s is the significant duration and T_m is the mean quadratic period as defined by Rathje *et al*. [11]. Figure 4 shows the elastic response spectra of the original and the scaled horizontal components compared with the building code spectrum, as well as the scaled acceleration time histories of a_x and a_y.

The free-field seismic response analyses were carried out assuming an elastic bedrock, by applying a time history of shear stress τ_{xy} at the base of the column:

$$\tau_{xy}(t) = \rho V_S \cdot \int a(t) \tag{2}$$

where ρ = 2.06 Mg/m^3 and V_S = 1000 m/s are the bedrock density and shear wave velocity, while $\int a(t)$ is the velocity obtained by integrating the horizontal component of the acceleration time history. FLAC "quiet" (viscous) boundary conditions were applied at the bottom of the grid while free-field boundary conditions were activated to the lat-

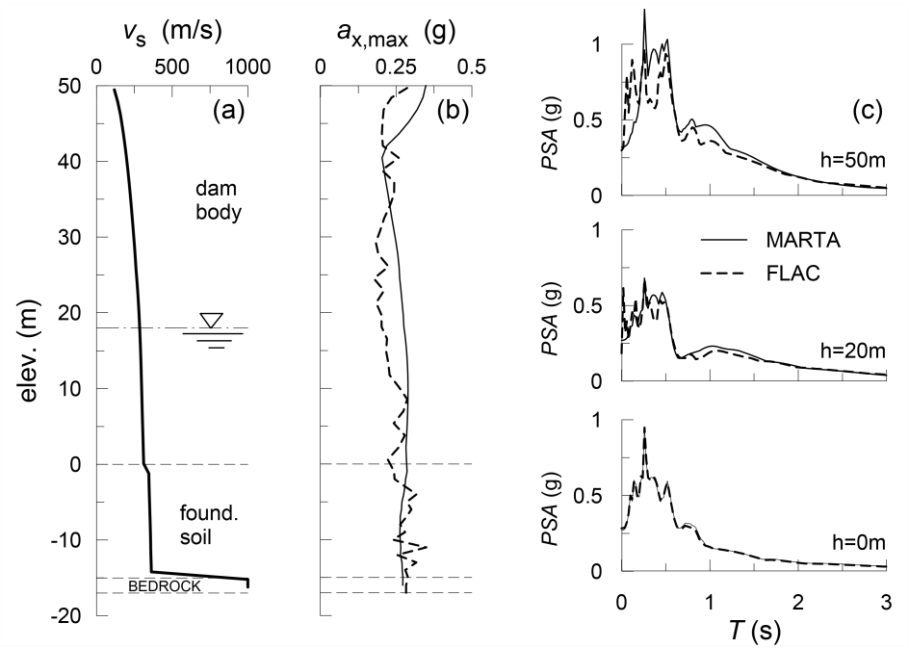

***Figure 5**. Results of free-field analyses.*

eral sides. The small-strain shear stiffness was also activated at the beginning of the dynamic analyses.

Figure 5 shows the results of FLAC 1D free-field analyses compared with those obtained using the code MARTA. The adopted shear wave velocity profile is shown in Figure 5a. Similar values of the maximum horizontal acceleration $a_{x,max}$ were computed with both methods, in the bedrock and the foundation soil (Figure 5b), while lower values were obtained in the dam body with the finite difference analysis, as the hysteretic model predicts a somewhat larger damping for $\gamma > 0.1$ %. Figure 5c shows the elastic response spectra computed at the base ($h = 0$ m), at about the middle ($h = 20$ m) and at the top ($h = 50$ m) of the dam body. The two methods are in a fair agreement to each other though the FLAC analysis tends to emphasise the high frequencies.

2.2. 2D simulations

Before the dynamic analyses, a pseudo-static analysis was carried out after completing the simulation of dam construction, in which a uniform horizontal body force was applied: it was expressed as a fraction k_h of gravity. The value of the seismic coefficient k_h was increased progressively until convergence, evidenced by a steady reduction of the unbalanced forces, became no longer possible. Under this circumstance, the numerical model exhibited a well-defined mechanism, associated with a plastic flow of the soil. The seismic coefficient k_h that activates the mechanism is termed 'critical' and is indicated as k_c. It was found [10] that the solution does not depend on the stiffness of the materials and therefore can be assumed to be a result of the strength properties only. Therefore, the critical seismic coefficient k_c represents a measure of the global seismic resistance of the system. Since the pseudo-static analyses were carried out up to critical conditions, the values of the computed displacements are only conventional, as they refer to a system that is accelerating due to the static activation of a plastic mechanism.

Calculations were conducted for both directions of the horizontal component of the inertial force $k_h \cdot g$, while the vertical component were kept constant. The minimum value of the critical seismic coefficient, $k_c = 0.212$, was obtained when the pseudo-static force is oriented towards the upstream slope. Figure 6 shows the deformed mesh computed for $k_h = k_c$. A plastic mechanism is activated from the top to the toe of the embankment, on the upstream side, mainly consisting in the rotation of the unstable soil mass.

Pseudo-static numerical analyses provide a first insight into the behaviour of the dam when subjected to intense seismic loading, capable of mobilising temporarily the soil shear strength. However, they are not able to take into account the transient nature of the earthquake action with inertial forces and internal states that change with time.

Starting from the end-of-construction stage, time-domain dynamic analyses were carried out by applying time-histories of the input motion to the bottom boundary of the same finite difference grid used for the pseudo-static analyses. For these analyses, FLAC "quiet" viscous

boundary conditions were activated to the lateral sides of the grid, and soil stiffness was set equal to the small strain stiffness.

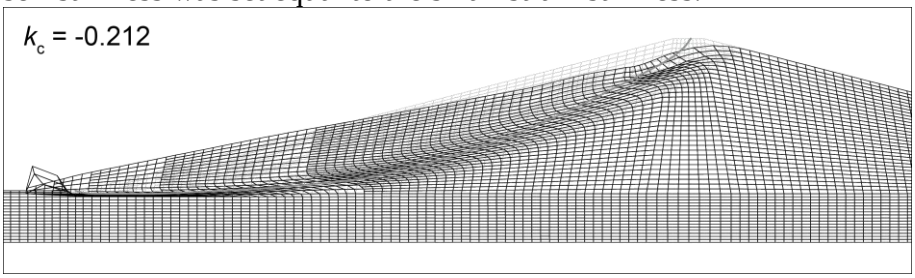

***Figure 6**. Pseudo static analysis, deformed mesh computed for $k_h = k_c$.*

Calculations were conducted for both the assumption of rigid and deformable bedrock. In the first case, time-histories of accelerations were applied to the bottom boundary, while, in the last case, time-histories of stresses were used. These were calculated using Eq. 2 for the horizontal component, while the vertical component was expressed as:

$$\sigma_{yy}(t) = \rho V_p \cdot \int a(t) \tag{3}$$

where V_p is the compression wave velocity at the bedrock, assumed equal to 2000 m/s. Both drained and undrained conditions were assumed in calculations. A water bulk modulus $K_w = 1$ GPa was assumed in the undrained analyses. In this paper only the results of the undrained analyses are shown. Specifically, four cases of analysis are discussed in the following: in two of them a rigid bedrock was assumed, neglecting (A) or considering (C) the vertical component of the input motion; calculations were repeated assuming a compliant elastic bedrock, in the absence (B) and the presence (D) of the vertical component of the seismic action.

Figure 7a shows the profiles of $a_{x,max}$ along the dam centre line. Nearly constant values were computed in the foundation soil while a deamplification is observed in the lower two-thirds of the embankment; in the topmost third $a_{x,max}$ increases to about twice the value obtained at the base as a result of seismic waves converging to the top of the dam.

The smallest values of $a_{x,max}$ were obtained assuming a compliant bedrock and neglecting the vertical component of the seismic action (B), while a 80% increment at the crest of the dam was calculated in the case of a rigid bedrock (A), or the one of a compliant bedrock in the presence of the vertical component of the input motion (D). Not surprisingly, therefore, for case C, that involves assumptions of rigid bedrock and presence of a_y, sensibly larger values of $a_{x,max}$ were computed both in the embankment and in the foundation soil.

Larger amplification effects were computed for the maximum values of the vertical acceleration $a_{y,max}$ (Figure 7b). In fact, assuming undrained conditions, the high bulk modulus of water, similar to that of the bedrock, results in a response of the system which is globally more rigid for compressive loadings, leading to a larger amplification of both the acceleration components.

It is worth mentioning that although considerably high values of $a_{x,max}$ and $a_{y,max}$ were computed, they are attained only for very short time intervals, and are usually associated to high frequencies and small energy contents.

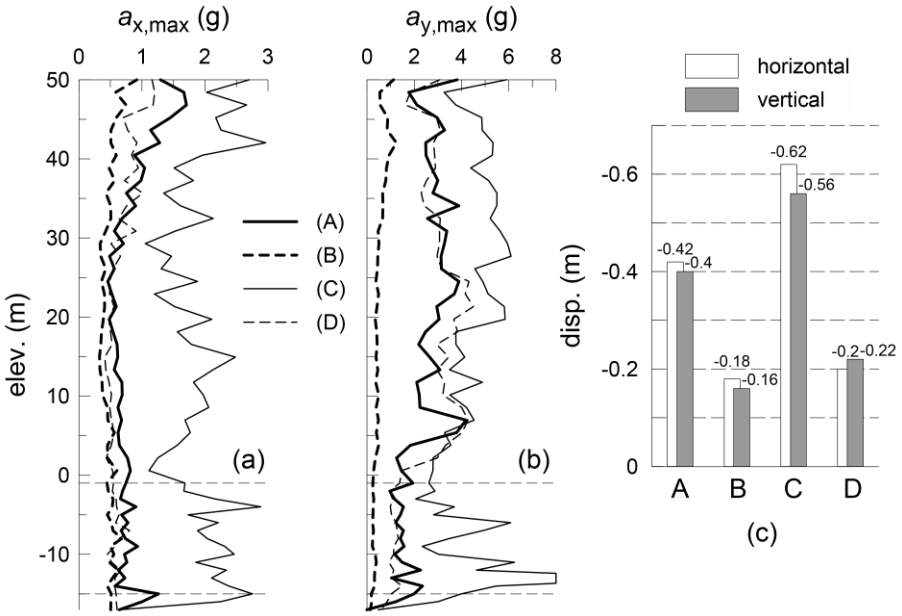

Figure 7*. Results of the 2D dynamic analyses.*

Figure 7c shows the maximum values of the horizontal (u) and of the vertical (w) displacement computed in the dam body. They were obtained in the upstream slope at about one-third of the dam height. Negative values indicate horizontal displacements directed towards the upstream slope and vertical displacements directed downwards. As observed for the acceleration profiles, the maximum values of u and w were calculated for case C (u_{max} = -0.62 m and w_{max} = -0.56 m), while for cases A, B and D a reduction of about 60% was observed for both u and w. For a T_R = 2475 years earthquake, the maximum settlements are always smaller than the available freeboard (2.6 m).

3. Conclusion

Monitoring data from an existing homogeneous earth dam have been used to calibrate a two-dimensional numerical model. Specifically, a match was searched between the dam settlements measured during construction and the computed values, to calibrate the model. The seismic performance of the dam was then evaluated through a series of dynamic analyses by applying an input motion compatible with the design spectrum specified by the construction code (D.M. 26/06/2014 [9]) for a return period of 2475 years. The results evidenced that the vertical component of the seismic action induces a sensible increase of seismic displacements, with values of the maximum acceleration about 2 to 3 times higher. This effect is decreased when a compliant bedrock is accounted for in the analysis. In spite of the high accelerations computed when considering the horizontal and vertical components of input motion, plastic mechanisms are activated only temporarily and the maximum final settlements resulted always lower than the available freeboard (2.6 m). Therefore, the dam is expected to perform satisfactorily in the presence of very intense seismic loadings.

Acknowledgements

The research work presented in this paper was partly funded by the Italian Department of Civil Protection under the ReLUIS 2014-2015 research project.

References

[1] Calabresi, G., Rampello, S., Sciotti, A., Amorosi, A., 2000, *Diga sulla Marana Capacciotti: verifica delle condizioni di stabilità e analisi del comportamento in condizioni sismiche*, Rapporto di Ricerca Università degli Studi di Roma La Sapienza, Dip. di Ingegneria Strutturale e Geotecnica. A cura e per conto del Consorzio per la Bonifica della Capitanata. Bastogi Editrice, Foggia.

[2] Cascone, E., Rampello, S.: Decoupled seismic analysis of an earth dam, *Soil Dynamics and Earthquake Engineering*, Vol.23 n.5, 2003, pp. 349-365.

[3] Amorosi, A., Elia, G: Analisi dinamica accoppiata della diga Marana Capacciotti, *Rivista Italiana di Geotecnica*, Patron editore, Bologna, Vol.52, n.4, 2008, pp. 78-95.

[4] Rampello, S., Cascone, E., Grosso, N.: Evaluation of the seismic response of a homogeneous earth dam, *Soil Dynamics and Earthquake Engineering*, Vol.29 n.5, 2009, pp. 782-798.

[5] Elia, G., Amorosi, A., Chan, A.H.C., Kavvadas, M.J.: Fully coupled dynamic analysis of an earth dam, *Géotechnique*, Vol.61 n.7, 2010, pp. 549-563.

[6] Itasca, 2005, *FLAC Fast Lagrangian Analysis of Continua v. 5.0*, User's Manual, Minneapolis, MN, USA: Itasca Consulting Group.

[7] Callisto, L., 2015, *MARTA v. 1.1: a computer program for the site response analysis of a layered soil deposit*, https://sites.google.com/a/uniroma1.it/luigicallisto/attivita-1.

[8] Ishibashi, I., Zhang, X.: Unified dynamic shear moduli and damping ratios of sand and clay, *Soils and Foundations*, Vol.33 n.1, 1993, pp. 182-191.

[9] Ministero delle Infrastrutture e dei Trasporti, 2014. *D.M. 26/06/2014, Norme tecniche per la progettazione e la costruzione degli sbarramenti di ritenuta (dighe e traverse)* Gazzetta ufficiale della Repubblica Italiana, Vol. 156.

[10] Masini, L, Callisto, L, Rampello, S.: An interpretation of the seismic design of reinforced-earth retaining structures, *Géotechnique*, Vol.65, n.5, 2015, pp:349–358, doi:http://dx.doi.org/10.1680geot./SIP 15-P-001.